Biosensors and Bioelectronics 24 (2008) 819–824

Contents lists available at ScienceDirect

Biosensors and Bioelectronics

journal homepage: www.elsevier.com/locate/bios

Direct electrochemistry of hemoglobin on carbonized titania nanotubes and its application in a sensitive reagentless hydrogen peroxide biosensor

Chunxian Guo[a,b,1], Fengping Hu[a,c,1], Chang Ming Li[a,b,*], Pei Kang Shen[c,**]

[a] School of Chemical and Biomedical Engineering, Nanyang Technological University, Singapore 637457, Singapore
[b] Center for Advanced Bionanosystems, Nanyang Technological University, Singapore 637457, Singapore
[c] State Key Laboratory of Optoelectronic Materials and Technologies, School of Physics and Engineering, Sun Yat-Sen University, Guangzhou 510275, PR China

ARTICLE INFO

Article history:
Received 9 April 2008
Received in revised form 2 July 2008
Accepted 3 July 2008
Available online 15 July 2008

Keywords:
Hemoglobin direct electrochemistry
Carbonized TiO_2 nanotubes
H_2O_2 biosensor of third generation

ABSTRACT

Carbonized TiO_2 nanotubes (TNT/C) prepared by carbonization with organic polymers possess advantages combined from high conductivity of carbon and nanostructure of TiO_2 nanotubes. The material was used as a supporting matrix to immobilize a redox protein, hemoglobin (Hb), to explore its direct electron transfer ability. The apparent heterogeneous electron transfer rate constant (k_{ET}) of Hb on TNT/C is 108 s^{-1}, which is much higher than that in the reported works, demonstrating excellent direct electrochemistry behavior. The TNT/C-Hb modified glassy carbon electrode (GCE) demonstrates significant electrocatalytic activity for reduction of hydrogen peroxide with a small apparent Michaelis–Menten constant (87.5 μM). The TNT/C-Hb based H_2O_2 sensor has a low detection limit (0.92 μM), fast response time (3 s) and high dynamic response range (10^{-6} to 10^{-4} M), a much better performance than the reported works. These results demonstrate that a direct electrochemistry behavior can be significantly enhanced through simple carbon coating on a nanostructured material for higher reaction surface area and better conductivity. This work suggests that Hb-immobilized TNT/C has potential applications in a sensitive H_2O_2 sensor.

1. Introduction

Direct electron transfer between biomolecules and electrode has been extensively studied because of its great importance in fundamental science in biological reactions (Wei et al., 2002), and broad applications in energy systems (Qiao et al., 2008a), bioelectronics (Tien et al., 1991), and biosensors (Cui et al., 2007; Salimi et al., 2007; Zang et al., 2007). The direct electrical communication between redox protein and electrode surface could particularly provide the way for superior mediator-free and sensitive biosensors, which can not only work at a sensing potential closer to the potential of the redox protein to eliminate interference reactions, but also simplify the detection system for less reagent and better stability (Zhang et al., 2008). Unfortunately, direct electrochemistry of most redox proteins on conventional electrodes is a great challenge due to the deeply buried redox-active center inside the proteins (Riklin et al., 1995).

Different approaches have been explored to enable the protein direct electrochemistry, such as physically adsorbed Hb on PSS/SWNT (Cheng et al., 2006), covalently bonded α-chymotrypsin in nanoporous sol–gel glass (Wang et al., 2001), and entrapped Hb on magnetic chitosan microspheres (Lai et al., 2008). Nanomaterials with unique structures can facilitate direct electron transfer due to their small size, novel physical, electronic and chemical properties for electron-mediating the redox reaction (McKenzie and Marken, 2003). Recently, numerous nanostructured metal oxides have attracted considerable interest in the bioanalytical area because of their large surface area, good biocompatibility, simple fabrication, and good chemical and physical stability (Lu et al., 2007; Bao et al., 2007). These materials, such as MnO_2 nanoparticles for glucose oxidase (Luo et al., 2004), MnO_2 nanosheet for myoglobin (Xiao et al., 2007), ZnO nanowires for GOD (Zang et al., 2007), zirconium dioxide nanoparticles for Hb (Liu et al., 2004), Co_3O_4 nanoflakes for Hb (Lu et al., 2007), nickel oxide nanoparticles for GOD (Salimi et al., 2007), and Fe_3O_4 nanoparticles for Hb (Cao and Hu, 2006), have good catalytic stability and activity, of which some are capable of direct electrochemistry (Liu et al., 2004; Cao and Hu, 2006). Various TiO_2 nanostructures such as TiO_2 anatase nanoparticles, nanotubes and nanosheets were used to immobilize proteins for studies of bioelectrocatalysis and direct electrochemistry (Liu et al., 2005; Zhang et al., 2007a), of which mesoporous TiO_2 can provide unique

* Corresponding author at: School of Chemical and Biomedical Engineering, Nanyang Technological University, Singapore 637457, Singapore. Tel.: +65 67904485; fax: +65 67911761.
** Corresponding author at: School of Physics and Engineering, Sun Yat-Sen University, Guangzhou 510275, PR China. Tel.: +86 20 84036736; fax: +86 20 84113369.
E-mail addresses: ecmli@ntu.edu.sg (C.M. Li), stsspk@mail.zsu.edu.cn (P.K. Shen).
[1] Authors have equal contributions.

0956-5663/$ – see front matter © 2008 Elsevier B.V. All rights reserved.
doi:10.1016/j.bios.2008.07.007

nanostructures with high specific surface area (Bao et al., 2007; Qiao et al., 2008a,b).

Accurate determination of H_2O_2 is of great importance because it is an essential mediator in food, pharmaceutical, clinical, industrial and environmental analyses. Direct electrochemistry of proteins on an electrode surface has been studied to sensitively detect H_2O_2 without the additional electron transfer mediator. Hb-immobilized MWNT (Qi et al., 2006), myoglobin entrapped in TiO_2 nanosheet (Zhang et al., 2007a) and Hb-modified zirconia nanoparticles-collagen matrix (Zong et al., 2007) were used to fabricate H_2O_2 sensors. However, there is a great need to further enhance the direct electron transfer rate of the mediatorless H_2O_2 sensor for not only further increasing the sensitivity, but also improving the response time, since the sensor often suffers from sluggish response time (longer than 5 s in most cases) due to its limited direct electron transfer rate between redox proteins and electrode (Wu et al., 2007).

TiO_2, one of the most widely used metal oxide materials in cosmetics, solar cells, batteries and paints, has demonstrated its excellent catalytic behaviors (Topoglidis et al., 2001). However, like other nanostructured metal oxide semiconductors, plain TiO_2 has poor conductivity and is not suitable for the direct electrochemistry. In our pervious works, great improvement of conductivity of TiO_2 has been achieved with carbon nanotube templated mesoporous TiO_2 (Bao et al., 2007) and polyaniline/TiO_2 nanocomposite (Qiao et al., 2008a, 2008b). In this work, a carbonized TiO_2 nanotube (TNT/C) synthesized by a uniform carbonization with organic polymers with enhanced conductivity and surface area is used to explore the direct electrochemistry of Hb and its applications for a mediator-free H_2O_2 biosensor.

2. Experimental

2.1. Reagents

Hb from bovine blood and hydrogen peroxide (30% (w/v) solution) was purchased from Sigma–Aldrich and used as received. Titania nanoparticles were purchased from Beijing Chemical, China. All the other chemicals were purchased from Sigma–Aldrich with analytical grade and used without further purifications.

2.2. Preparation of TNT and TNT/C

TNTs were synthesized from titania nanoparticles by a mild hydrothermal method as reported (Seo et al., 2001). TNT/C was prepared by carbonization of TNT with the organic polymer (Hu et al., 2006). In our work, TNT/C was fabricated by the following procedure. A mixture of 50.0 mg TiO_2 nanotubes and 94.7 mg poly(ethylene glycol) 600 was placed in a quartz tube, through which Ar flowed at 500 sccm for 60 min before heating. Then the flow rate of Ar was decreased to 100 sccm and the mixture was heated for 30 min at 600 °C.

2.3. Electrode modification

Glass carbon electrodes with 3 mm in diameter (GCE, CH Instruments, USA) were polished with 0.3 and 0.05 μm alumina powder sequentially, followed by thoroughly rinsing with deionized water. After sonicating in acetone and then in deionized water, the electrodes were dried at room temperature. Protein immobilizations of TNT and TNT/C were conducted by immersing 10 mg of these materials in 1 mL Hb solution (10 mg mL^{-1}, pH 7.4, 0.01 M PBS), respectively under ambient conditions while shaking for half an hour, followed by storage at 4 °C overnight for protein adsorption. Then, the solution became a suspension and was ready for use. For every use, the suspension was re-shaken, of which 5 μL was taken and dropped onto the surface of the pretreated GCE, followed by drying at room temperature, and then 3 μL Nafion (0.5% aqueous) solution was dropped above to form a Nafion membrane. For electrochemical characterization of as-prepared materials, the electrodes were prepared without Nafion coating by casting 5 μL of TNT or TNT/C (10 mg mL^{-1} in distilled water) on the pretreated GCE, following by drying under ambient conditions.

2.4. Apparatus and measurements

Morphology and microstructure of the synthesized materials were examined by field emission scanning electron microscopy (FESEM, JSM-6700F, Japan). Electrochemical measurements were carried out with a three-electrode system, employing a platinum wire, a saturated calomel electrode (SCE), and a TNT or TNT/C electrode with or without immobilization of protein and Nafion as counter, reference and working electrode, respectively. Before experiments, the buffer solution was bubbled with pure nitrogen for a thoroughly anaerobic condition. All measurements were performed at room temperature.

3. Results and discussion

3.1. Morphology characterization of TNT and TNT/C

The FESEM image of Fig. 1a illustrates that the TNT has a highly loose bundle structure. A typical TEM image of TNT is shown in the inset of Fig. 1a, from which the hollow nature of the nanotubes can be clearly observed. The inner diameter, outside diameter and length of the TNT range from 15 to 20 nm, 20 to 30 nm and 1 to 5 μm, respectively. The TNT/C still retains the highly loose bundle structure (Fig. 1b), but is more uniform and more porous than TNT. The size of TNT/C bundle is around 50 nm, which is slightly larger than TNT. Clearly, the carbonization of TNT enhances the porosity to increase its specific surface area, very likely due to the additional, porous thin layer of carbon on the TNT surface.

3.2. Electrochemical activity of TNT and TNT/C

The electrochemical activities of TNT and TNT/C were characterized by electrochemical impedance spectroscopy (EIS) and cyclic voltammetry (CV) of 10 mM $Fe(CN)_6^{-3}$ in 1.0 M KCl and the results are shown in Fig. 2. The measured complex impedance (Z) versus frequency, known as Nyquist Plot is shown in Fig. 2a, in which well-defined frequency-dependent semicircle impedance curves are observed at the high frequency range followed by a straight line. The diameter of the semicircle for TNT/C is much smaller than that for TNT. Randle equivalent circuit is often used to model the complex impedance in an electrochemical cell, which is composed of the ohmic resistance of the electrolyte solution, R_s in connection in series with parallel elements of double layer capacitance, C_{dl}, and Faraday impedance, Z_f. The parallel elements C_{dl} and Z_f versus frequencies form a semicircle over a high frequency range, and Z_f often comprises serially connected charge transfer resistance, R_{ct}, which determines the diameter of the semicircle and Warburg impedance, Z_w from the diffusion of ions in the bulk electrolyte to the electrode surface. The values of R_{ct} obtained from Fig. 2a are 98 and 19.6 Ω cm^2 for TNT and TNT/C electrode, respectively, indicating that TNT/C modified GCE has much higher conductivity than that of TNT modified GCE.

Exchange current density (i_0) and standard rate constant (k^0) are used to evaluate the electrocatalytic performance of an electrode material. The larger the exchange current density and standard rate constant are, the better the electrocatalysis is. i_0 and k^0 can be

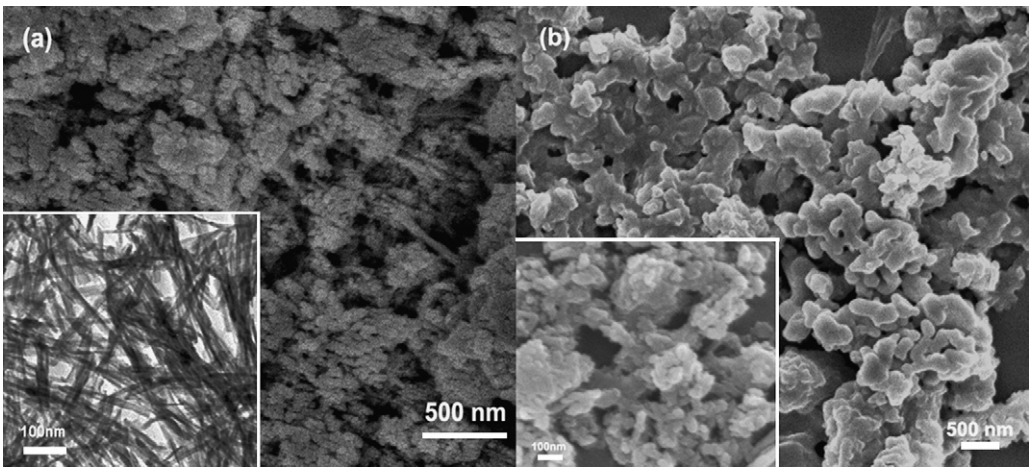

Fig. 1. FESEM image of TNT (a) and TNT/C (b). Inset of (a) is TEM of TNT and inset of (b) is the high-magnification FESEM of TNT/C.

calculated from R_{ct} by using Eq. (1) and Eq. (2), derived from the Butler–Volmer relationship of current and potential (Zhang and Rusling, 1997).

$$i_0 = \frac{RT}{FR_{ct}} \quad (1)$$

$$k^0 = \frac{i_0}{FC} \quad (2)$$

where R, T, F and C are gas constant, absolute temperature, Faradic constant and concentration of the reactant, respectively. The calculated i_0s are 2.62×10^{-4} and 1.31×10^{-3} A cm^{-2} for TNT and TNT/C, respectively, while the calculated k^0s are 2.72×10^{-3} s^{-1} and 1.36×10^{-2} s^{-1} for TNT and TNT/C, respectively, indicating much faster charge transfer rate of TNT/C than TNT.

The CVs in Fig. 2b show that the electrochemical redox reaction of $Fe(CN)_6^{3-/4-}$ on the TNT/C electrode has much higher peak current and smaller peak potential separation than that on TNT electrode, indicating the former is more reversible than the latter. The results here further support that the carbon coating on TiO_2 can improve the reversibility of its catalyzed electrochemical reactions. However, although the cathodic peak current equals to its corresponding anodic one on both electrode surface, their peak potential separations are larger than 59.5 mV. This is likely ascribed to their quasi-reversible reaction nature. The electrochemically active surface area can be estimated according to the following equation for an quasi-reversible process (Hrapovic et al., 2007),

$$i_p = (2.99 \times 10^5) n(\alpha n_a)^{1/2} ACD^{1/2} \upsilon^{1/2} \quad (3)$$

Assuming $\alpha = 0.5$ and $n_a = 1$, where n, A, D, υ and C are the number of electrons involved in the reaction, the electrochemically active surface area, the diffusion coefficient of the reactant species in solution (cm^2 s^{-1}), the scan rate of the potential perturbation (V s^{-1}) and the concentration of the reactant in the bulk solution (mol cm^{-3}), respectively. The redox reaction of $Fe(CN)_6^{3-/4-}$ involves one-electron transfer ($n = 1$) and the diffusion coefficient (D) is 6.30×10^{-6} cm^2 s^{-1} (Hrapovic et al., 2007). The value of the electrochemically active surface area for TNT/C modified GCE is 7.5×10^{-2} cm^2 in terms of the calculation from Eq. (3), which is larger than that of TNT (3.4×10^{-2} cm^2) by two times. The larger reaction surface area should come from its higher specific surface area after carbonization. The results discussed above demonstrate that the improvement of the electrocatalysis of TNT/C is produced by both reaction surface area and charge transfer rate.

3.3. Direct electrochemistry of TNT-Hb and TNT/C-Hb

The direct electrochemistry behavior of Hb on both TNT/C and TNT was studied. Fig. 3 shows CVs obtained from the TNT/C, TNT/C-Hb, TNT and TNT-Hb modified GCEs in pH 5.0 acetate buffer. There is no reaction peak current observed for TNT/C or TNT modified GCEs

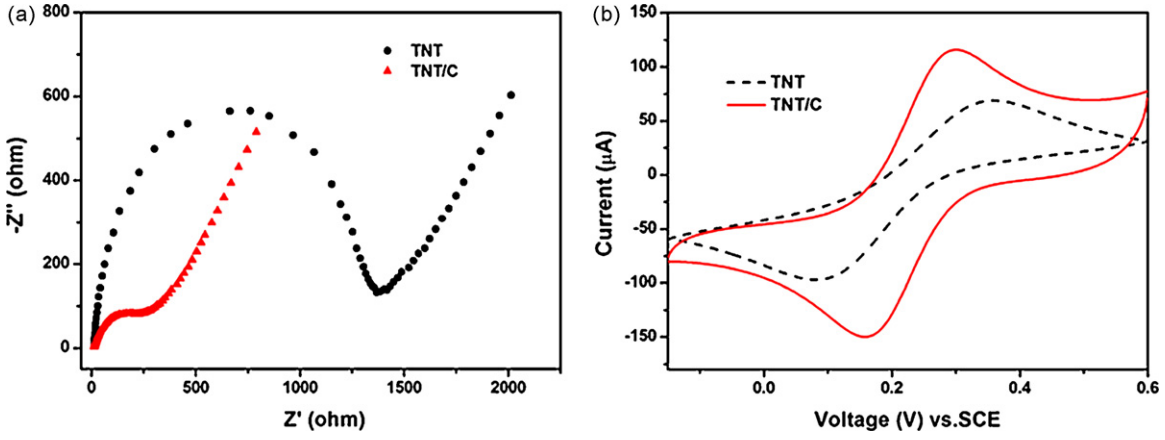

Fig. 2. (a) EIS and (b) CV of 10 mM $Fe(CN)_6^{3-/4-}$ in 1.0 M KCl using TNT and TNT/C modified GCE.

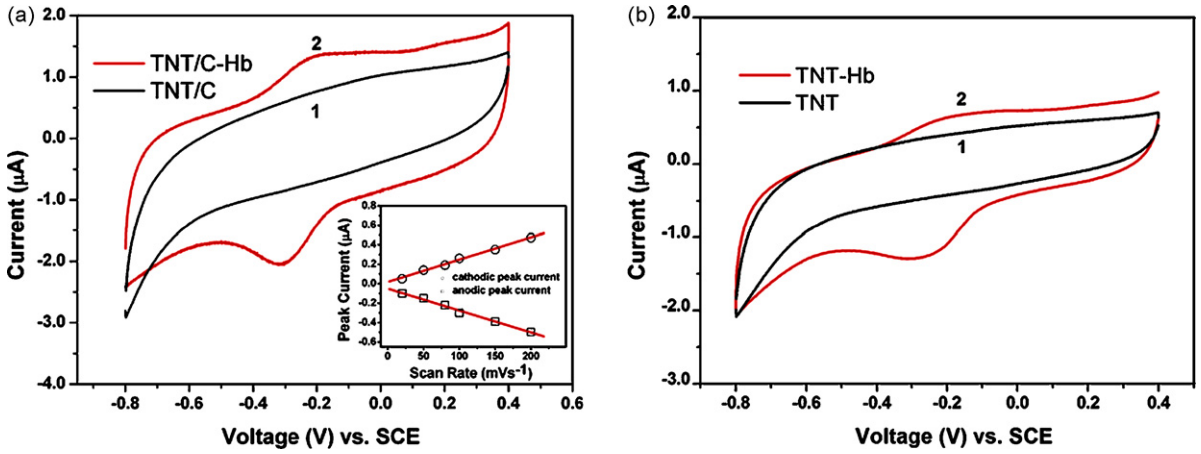

Fig. 3. CVs of (a) TNT/C and TNT/C-Hb modified GCEs, (b) TNT and TNT/Hb modified GCEs in 0.1 M pH 5.0 acetate buffer solutions at 100 mV s^{-1}, and inset of (a) is the plot of anodic and cathodic peak currents of TNT/C-Hb electrode versus the scan rate (20, 50, 80, 100, 150, and 200 mV s^{-1}).

within the potential window (curve 1 in Fig. 3a and b). However, quasi-reversible reaction behavior is illustrated for both TNT/C-Hb and TNT-Hb as in curve 2 of Fig. 3a and b, respectively, in which the TNT/C-Hb has much higher reversibility of direct electrochemistry than the TNT-Hb in terms of its much more prominent redox peak current and more symmetric redox wave than that of TNT-Hb. The peak-to-peak separation (ΔE_p) is 42.6 mV at scan rate 100 mV s^{-1}, which is smaller than 62.5 mV for Hb in mesoporous silica matrix (Dai et al., 2004) and 58.6 mV for Hb in Fe_3O_4 nanoparticles (Cao and Hu, 2006) observed at the same scan rate, indicating more reversible behavior for faster electron transfer of Hb than the reported literatures can be achieved. Both cathodic and anodic peak current of CVs obtained from TNT/C-Hb is linearly proportional with scan rate from 20 mV s^{-1} to 200 mV s^{-1}, as shown in the inset of Fig. 3a, indicating an electrochemical redox reaction of a surface immobilized species and further proving the direct electrochemistry nature of Hb on the TNT/C surface.

The effects of ratio of Hb to TNT/C by weight ($W_{Hb}/W_{TNT/C}$) and the total amount of TNT/C-Hb on the direct electrochemistry behavior were studied. When the $W_{Hb}/W_{TNT/C}$ ratio increases, the peak current increases until the ratio is up to 1:10 (1 mg mL^{-1}:10 mg mL^{-1}), at which the current becomes almost constant (data not shown). The peak current also increases with the increase of the total amount of TNT/C-Hb while keeping a constant $W_{Hb}/W_{TNT/C}$ = 1:10; however, no significant effect is observed after 7.08×10^{-4} g cm^{-2} of TNT/C-Hb is immobilized. This possibly implies that only the Hb molecules near the electrode surface in a thin layer of TNT/C could undergo direct electrochemistry. Therefore, 7.08×10^{-4} g cm^{-2} of TNT/C-Hb with $W_{Hb}/W_{TNT/C}$ ratio of 1:10 was chosen for further studies.

Square wave voltammetry (SWV), which has better signal-to-noise ratio than CVs, was often used to estimate the apparent heterogeneous electron transfer rate constant (k_{ET}) (Fan et al., 2001). The method employs nonlinear regression to analyze SWV with the single-species thin-layer SWV model (Zhou et al., 2002). SWVs measured with TNT/C-Hb and TNT-Hb electrodes are shown in Fig. 4a, from which the average k_{ET} values of Hb in TNT/C and TNT obtained are 108 and 72 s^{-1}, respectively. The k_{ET} value (108 s^{-1}) of Hb on TNT/C is much larger than Hb on TNT and significantly greater than that on Fe_3O_4 nanoparticles (25 s^{-1}), clay film (38 s^{-1}), and on SiO_2 nanoparticle film (76 s^{-1}) (Cao and Hu, 2006) as well. This demonstrates excellent direct electrochemistry of Hb on the TNT/C surface, and could be attributed to its novel nanostructure and good conductivity for allowing fast direct electron transfer of Hb.

3.4. Effect of solution pH on the direct electrochemistry of Hb on TNT/C

The direct electrochemistry of TNT/C-Hb modified GCEs shows a strong dependence on solution pH as shown in Fig. 4b. Voltammograms with well-defined peaks were measured in the range of 3.0–7.0. Negative shifts in both anodic and cathodic peak potentials are observed with pH increase and the changes are very reversible. The formal potential (E_p) is found to be linearly decreasing with a slope of −62.5 mV/pH when increasing pH from 3.0 to 7.0 (inset of Fig. 4b), which is close to the expected theoretical value of −57.6 mV/pH for a reversible proton-coupled single electron transfer process, suggesting that a single protonation accompanies electron transfer between the electrode and each of the four heme-Fe^{III}s of Hb (Sakamoto et al., 2004). The pH value also affects the redox peak currents of Hb (Fig. 4b). Obviously, the maximum peak currents are observed at pH value ~5.0. This may indicate that the assembled Hb has its highest bioactivity around the pH 5.0 value.

3.5. Electrocatalysis of the TNT-C/Hb towards sensitive H_2O_2 detection

Hemoglobin possesses an intrinsic peroxidase activity due to its similarity with peroxidase for catalysis of reduction of H_2O_2 (Sakamoto et al., 2004). The electrocatalytic properties of the TNT/C-Hb toward H_2O_2 reduction were investigated by cyclic voltammetry. As shown in Fig. 5a, at the TNT/C-Hb modified GCE, the reduction (cathodic) peak current at around −0.35 V increases significantly with increase of H_2O_2 concentration (curves 3–7) accompanying the disappearance of the oxidation (anodic) peak current, demonstrating a typical electrocatalytic reduction process of H_2O_2. However, no peak is observed at the TNT/C modified GCE in the presence of H_2O_2, showing no reduction of H_2O_2 occurs at the TNT/C modified GCE (curve 2). Apparently, the H_2O_2 reduction is due to electrocatalysis from Hb–Fe^{II} of Hb, which can reduce H_2O_2 while being oxidized to Hb–Fe^{III} and then quickly reduced back to Hb–Fe^{II} through its direct electron transfer ability with the electrode (Zhang et al., 2007b).

The H_2O_2 reduction on TNT/C-Hb was explored for an amperometric H_2O_2 sensor. Fig. 5b displays the amperometric responses of different concentrations of H_2O_2 at TNT/C-Hb modified GCE with an applied potential of −0.35 V versus SCE in acetate buffer (pH 5.0). During the measurement, the concentration change of H_2O_2 in the buffer was conducted by addition of H_2O_2 every 40 s. The injected H_2O_2 caused a stepped increase in reduction current,

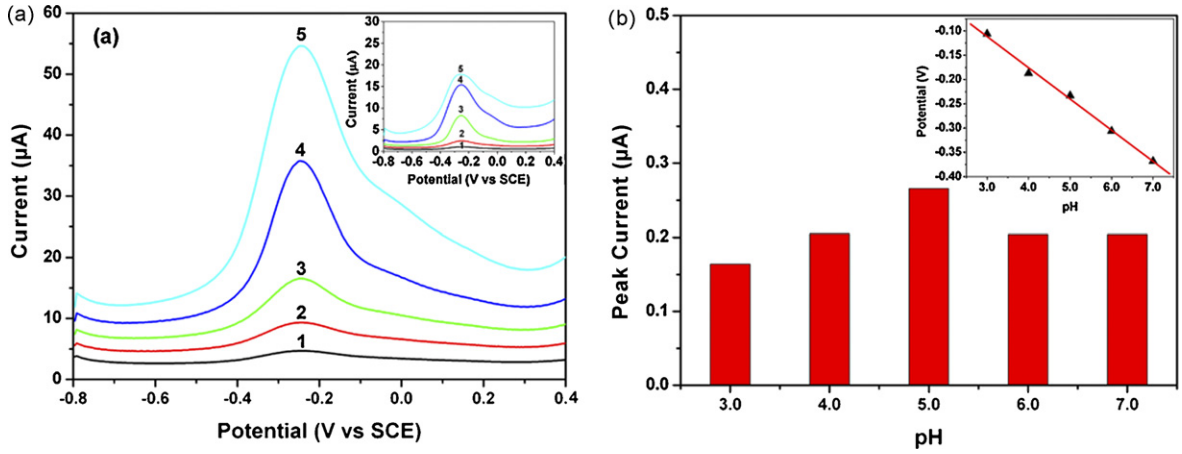

Fig. 4. (a) SWV of TNT/C-Hb in 0.1 M pH 5.0 acetate buffer solution and inset of (a) is TNT-Hb covered GCE. SWV conditions: equilibrium time, 5 s; potential amplitude, 100 mV; step height, 4 mV and frequency, 10 (1), 20 (2), 30 (3), 40 (4), and 50 Hz (5). (b) Plot of peak current versus pH value and inset of (b) is the plot of formal potential versus pH.

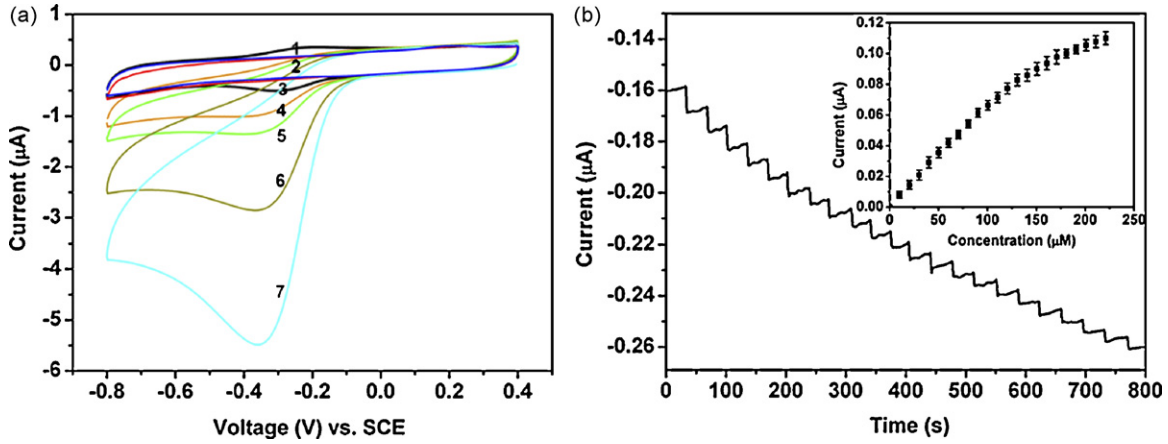

Fig. 5. (a) CVs of TNT/C-GCE in 0.1 M acetate buffer solution (pH 5.0) with (1) 0 and (2) 1 mM H_2O_2; CVs of TNT/C-Hb-GCE in 0.1 M acetate buffer with (3) 0, (4) 0.1, (5) 0.2, (6) 0.5, and (7) 1 mM H_2O_2;. Scan rate: 100 mV s^{-1}. (b) Current–time curve of the TNT/C-Hb-GCE measured in different concentrations of H_2O_2 in 0.1 M acetate buffer at −0.35 V; inset: calibration curve of the sensor.

which is in good agreement with the CV results shown in Fig. 5a. From the steady-state measurements, the response time of less than 3 s was determined when the responding current reaches 95% of the steady-state current, which is much faster than Hb-based H_2O_2 sensors (>5 s) (Liu et al., 2004; Yang et al., 2007). The response linear range was up to 1.60×10^{-4} M with a detection limit of 0.92×10^{-6} M for a signal-to-noise ratio of 3. The higher sensitivity and faster catalytic response of TNT/C-Hb electrode can be attributed to the good direct electrochemistry behavior of Hb on TNT/C.

The apparent Michaelis–Menten constant (K_M), an indication of the enzyme–substrate kinetics, is generally used to evaluate the biological activity of an immobilized enzyme (Bao et al., 2007). When the concentration of H_2O_2 is higher than 1.60×10^{-4} M, the calibration curve tends to a plateau, showing a characteristic Michaelis–Menten kinetics mechanism of an enzymatic reaction (inset of Fig. 5b) (Njagi and Andreescu, 2007). K_M can be obtained by analysis of the slope and the intercept of the plot of the reciprocals of the steady-state current versus H_2O_2 concentration. In this work, the apparent Michaelis–Menten constant (K_M) was found to be 87.5 μM which is smaller than that of 112 μM for Nafion/CdS-Hb/GP electrode, 550 μM for membrane-entrapped HRP, and 230 μM for a HRP/Au colloid self-assembled monolayer electrode (Xu et al., 2007). The small apparent Michaelis–Menten constant shows a high affinity to H_2O_2 and good bioactivity of TNT/C-Hb toward H_2O_2 reduction.

As a sensor application of TNT/C-Hb, the stability is very critical, which was tested by continuous CV measurements for 3 h and the amperometric response reduced less than 2.5%. The TNT/C-Hb modified GCE sensor was stored in dry condition at 4 °C. It could retain 95% of its initial amperometric response after storage for two weeks. The stability testing results demonstrate that the TNT/C-Hb based H_2O_2 has good long-term storage life time, and sustains relatively long detection time (3 h) without significant drift, and then indicates its great potential application for a mediatorless H_2O_2 sensor.

4. Conclusions

Carbonized TiO_2 nanotubes (TNT/C) with highly porous and uniform nanostructure were prepared by carbonization with organic polymers. A comparative study between TNT/C and TNT demonstrates that TNT/C has higher conductivity, larger electrochemical active surface area and faster direct electron transfer rate for immobilized Hb. The TNT/C-Hb modified GCE has a high electrocatalytic activity on H_2O_2 reduction and is used for H_2O_2 sensor, which has lower detection limit (0.92 μM) and much faster response (3 s) than reported works. The sensor also has high dynamic response

range and good stability. The work reported here demonstrates that a direct electrochemistry behavior can be significantly enhanced through simple carbon coating on a nanostructure material and also renders a great potential application in mediator-free H_2O_2 detection.

Acknowledgment

This work is financially supported by Singapore A*STAR grant under Contract No. 052 117 003.

References

Bao, S.J., Li, C.M., Zang, J.F., Cui, X.Q., Qiao, Y., Guo, J., 2007. Adv. Funct. Mater. 18 (4), 591–599.
Cao, D.F., Hu, N.F., 2006. Biophys. Chem. 121 (3), 209–217.
Cheng, W.X., Jin, G.Y., Zhang, Y.Z., 2006. Sens. Actuators B Chem. 114 (1), 40–46.
Cui, X.Q., Li, C.M., Zang, J.F., 2007. Biosens. Bioelectron. 22 (12), 3288–3292.
Fan, C.H., Wang, H.Y., Sun, S., Zhu, D.X., Wagner, G., Li, G.X., 2001. Anal. Chem. 73 (13), 2850–2854.
Hrapovic, S., Liu, Y.L., Luong, J.H.T., 2007. Anal. Chem. 79 (2), 500–507.
Hu, F.P., Ding, F.W., Song, S.Q., Shen, P.K., 2006. J. Power Sources 163 (1), 415–419.
Lai, G.S., Zhang, H.L., Han, D.Y., 2008. Sens. Actuators B Chem. 129 (2), 497–503.
Liu, A.H., Wei, M.D., Honma, I., Zhou, H.S., 2005. Anal. Chem. 77 (24), 8068–8074.
Liu, S.Q., Dai, Z.H., Chen, H.Y., Ju, H.X., 2004. Biosens. Bioelectron. 19 (9), 963–969.
Lu, X.B., Zou, G.F., Li, J.H., 2007. J. Mater. Chem. 17 (14), 1427–1432.
Luo, X.L., Xu, J.J., Zhao, W., Chen, H.Y., 2004. Biosens. Bioelectron. 19 (10), 1295–1300.
McKenzie, K.J., Marken, F., 2003. Langmuir 19 (10), 4327–4331.
Njagi, J., Andreescu, S., 2007. Biosens. Bioelectron. 23 (2), 168–175.
Qi, H.L., Zhang, C.X., Li, X.R., 2006. Sens. Actuators B Chem. 114 (1), 364–370.
Qiao, Y., Bao, S.J., Li, C.M., Cui, X.Q., Lu, Z.S., Guo, J., 2008a. ACS Nano. 2 (1), 113–119.
Qiao, Y., Li, C.M., Bao, S.J., Lu, Z.S., Hong, Y.H., 2008b. Chem. Commun. 11, 1290–1292.
Riklin, A., Katz, E., Williner, I., Stockerand, A., Buckmann, A.F., 1995. Nature 376 (6542), 672–675.
Sakamoto, A., Sakurao, S., Fukunaga, K., Matsubara, T., Ueda-Hashimoto, M., Tsukamoto, S., Takahashi, M., Morikawa, H., 2004. FEBS Lett. 572 (1–3), 27–32.
Salimi, A., Sharifi, E., Noorbakhsh, A., Soltanian, S., 2007. Biosens. Bioelectron 22 (12), 3146–3153.
Seo, D.S., Lee, J.K., Kim, H., 2001. J. Cryst. Growth 229, 428–432.
Tien, H.T., Salamon, Z., Ottova, A., 1991. Crit. Rev. Biomed. Eng. 18 (5), 323–340.
Topoglidis, E., Campbell, C.J., Cass, A.E.G., Durrant, J.R., 2001. Langmuir 17 (25), 7899–7906.
Wei, J.J., Liu, H.Y., Dick, A.R., Yamamoto, H., He, Y.F., Waldeck, D.H., 2002. J. Am. Chem. Soc. 124 (32), 9591–9599.
Wang, P., Dai, S., Waezsada, S.D., Tsao, A., Davison, B.H., 2001. Biotechnol. Bioeng. 74 (3), 249–255.
Wu, S., Ju, H.X., Liu, Y., 2007. Adv. Funct. Mater. 17 (4), 585–592.
Xiao, H., Chen, X., Ji, L.Y., Zhang, X., Yang, W.S., 2007. Chem. Lett. 36 (6), 772–773.
Xu, Y.X., Liang, J.G., Hu, C.G., Wang, F., Hu, S.S., He, Z.K., 2007. J. Biol. Inorg. Chem. 12 (3), 421–427.
Yang, M.H., Qu, F.L., Li, Y.J., He, Y., Shen, G.L., Yu, R.Q., 2007. Biosens. Bioelectron. 23, 414–420.
Zang, J.F., Li, C.M., Cui, X.Q., Wang, J.X., Sun, X.W., Dong, H., Sun, C.Q., 2007. Electroanalysis 19 (9), 1008–1014.
Zhang, L., Zhang, Q., Li, J.H., 2007a. Adv. Funct. Mater. 17 (12), 1958–1965.
Zhang, R.Y., Wang, X.M., Shiu, K.K., 2007b. J. Colloid Interface Sci. 316 (2), 517–522.
Zhang, X.J., Ju, H.X., Wang, J., 2008. Electrochemical Sensors, Biosensors and Their Biomedical Applications. Elsevier, New York.
Zhang, Z., Rusling, J.F., 1997. Biophys. Chem. 63 (2–3), 133–146.
Zhou, Y.L., Hu, N.F., Zeng, Y.H., Rusling, J.F., 2002. Langmuir 18 (1), 211–219.
Zong, S.Z., Cao, Y., Zhou, Y.M., Ju, H.X., 2007. Anal. Chim. Acta 582 (2), 361–366.